

Nonequilibrium Transport in Superconductor/Ferromagnet/Superconductor Diffusive Junctions: Interplay between Proximity Effect and Ferromagnetism.

I. V. Bobkova and A. M. Bobkov

Institute of Solid State Physics, Chernogolovka, Moscow reg., 142432 Russia

(Dated: December 2, 2018)

The theory of the I-V characteristics in diffusive superconductor/weak ferromagnet/superconductor (SFS) junction is developed. We show that the exchange field h of the ferromagnet manifests itself as an additional conductance peak at $eV \sim \Delta + h$ in the phase-coherent regime, when the Thouless energy is of the order of superconducting order parameter. The excess current exhibits non-monotonous dependence on the exchange field and non-trivial temperature behavior, which is strongly influenced by the temperature dependence of the exchange field.

PACS numbers: 74.45.+c, 74.50.+r

The recent progress in the experimental techniques has made possible the fabrication of mesoscopic structures on the nanometer scale. Hybrid structures containing superconducting and ferromagnetic elements offer an opportunity to generate and control coherent spin transport with otherwise conventional electronics. The equilibrium transport and proximity effect in such structures have been theoretically and experimentally investigated recently in details as for the case of weak ferromagnetic alloys so as for half-metals like CrO_2 ^{1,2}. In particular, Josephson current in SFS junctions and T_c of SF bilayers and multilayers have been investigated in details for the case of weak ferromagnetic alloys (see Ref.3 and references therein). Equilibrium density of states was also studied^{4,5}. On the other hand, to the best of our knowledge, the nonequilibrium transport in SFS mesoscopic junctions has not been studied yet neither from theoretical nor from experimental point of view except for theoretical investigations of magnetic quantum point contacts^{6,7,8,9}. We address our theoretical paper to the part of this problem and study the phase-coherent transport in diffusive voltage-biased SFS plane junctions. We consider interlayers made of a weak ferromagnetic material, in which the value of the exchange field h (measured in the energy units) is of order of superconducting order parameter Δ . In ferromagnetic alloys like $CuNi$, which have been intensively used by now for experimental investigation of equilibrium properties of SFS heterostructures, the exchange field is several times larger than Δ . On the other hand, it can be concluded from our analysis of the problem that for studying the I-V characteristics of SFS junctions, made on the basis of a weak ferromagnetic alloy, the most interesting case is $h \lesssim \Delta$. As far as we know, the work on the creation of appropriate alloys is in progress now, so we believe that this limit can be experimentally realized in the nearest future.

The I-V characteristics of the superconductor/normal metal/superconductor (SNS) voltage-biased diffusive junction are studied theoretically in details mainly in two limits. The first one is the limit of short junction $d \ll \xi$, where d is the length of the interlayer, $\xi = \sqrt{\hbar D / \Delta}$ is the superconducting coherence length and D is the diffusion constant. In this regime the subharmonic gap structure

(SGS) in the differential conductance dI/dV consists of a set of pronounced maxima at $eV_n = 2\Delta/n$ ^{10,11}. The excess current, which takes place at high biases $eV \gg \Delta$, behaves in dependence on temperature as $\Delta(T)$ does and can be as positive so as negative depending on the transparency of SN interfaces^{10,12}. The second one is the incoherent limit $d \gg \xi$. The proximity effect is negligible in this regime and the transport is determined by the kinetic equation for the distribution function^{13,14,15}. The SGS of the conductance again shows sharp features at $eV_n = 2\Delta/n$. At the same time in the intermediate regime $\xi \sim d$ the proximity effect, which manifests itself as a minigap Δ_g in the equilibrium density of states in the normal region, takes place. It has been shown very recently¹⁶ that for SNS voltage-biased diffusive junction with highly-transparent NS interfaces in this regime, when the interplay between proximity effect and MARs takes place, the well-known subgap conductance structure $eV_n = 2\Delta/n$ modifies and exhibits an additional maximum at roughly $eV \sim \Delta + \Delta_g$. These predictions are in good agreement with the existing experiments^{17,18}. In the present work we numerically calculated the I-V characteristics taking into account the proximity effect and non-equilibrium distribution function in the ferromagnetic interlayer. We show that in the phase-coherent regime, when the proximity effect in the ferromagnetic region takes place, the exchange field of a weak ferromagnet $h < \Delta$ explicitly manifests itself in the SGS of diffusive voltage-biased SFS junction leading to the additional maximum at $eV \sim (\Delta + h)$, which is the most pronounced in the case of low-transparent SF boundaries. For the case $h > \Delta$ the differential conductance exhibits no pronounced characteristic features. The dc current at high voltage biases is also investigated. It is deficit ($I_{def} = I - V/R < 0$) for the case of highly-resistive interfaces we consider and has a non-monotonous behavior as a function of exchange field, reaching the maximum value at roughly $h \sim \Delta$. This non-monotonous behavior results in the fact, that the temperature dependence of the deficit current exhibits the characteristic features, which are determined by the temperature dependence of the exchange field and can be used for its experimental mapping.

Further the model under consideration and the method we use are briefly described. We study an SFS junction, where F is a diffusive weak ferromagnet of length d coupled to two identical superconducting (S) reservoirs. The superconductors are supposed to be diffusive and have s -wave pairing. We assume the SF interfaces to be not fully transparent and suppose that the resistance of the SF boundary R_g dominates the resistance of the ferromagnetic interlayer R_F . We use the quasiclassical theory of superconductivity for diffusive systems in terms of time-dependent Usadel equations¹⁹. The

fundamental quantity for diffusive transport is the momentum average of the quasiclassical Green's function $\check{g}(x, \varepsilon, t) = \langle \check{g}(\mathbf{p}_f, x, \varepsilon, t) \rangle_{\mathbf{p}_f}$. It is a 8×8 matrix form in the product space of Keldysh, particle-hole and spin variables. Here x - is the coordinate measured along the normal to the junction, t stands for a time variable and ε is the excitation energy.

The electric current should be calculated via Keldysh part of the quasiclassical Green's function. For the plane diffusive junction the corresponding expression reads as follows

$$\frac{j^{\text{el}}}{e} = -\frac{d}{8\pi^2 e^2 R_F} \int_{-\infty}^{+\infty} d\varepsilon \text{Tr}_4 \left[\frac{1}{2} (\hat{\tau}_0 + \hat{\tau}_3) \hat{\sigma}_0 \left(\check{g}(x, \varepsilon, t) \otimes \frac{\partial \check{g}(x, \varepsilon, t)}{\partial x} \right)^K \right], \quad (1)$$

where e is the electron charge and $\hbar = 1$ throughout the paper. $(\check{g}(x, \varepsilon, t) \otimes (\partial \check{g}(x, \varepsilon, t))/(\partial x))^K$ is a 4×4 Keldysh part of the corresponding combination of full Green's functions. The product \otimes of two functions of energy and time is defined by the noncommutative convolution $A \otimes B = e^{i(\partial_\varepsilon^A \partial_t^B - \partial_t^A \partial_\varepsilon^B)} A(\varepsilon, t) B(\varepsilon, t)$. $\hat{\tau}_i$ and $\hat{\sigma}_i$ are Pauli matrices in particle-hole and spin spaces respectively.

The quasiclassical Green's function $\check{g}(x, \varepsilon, t)$ satisfies the non-stationary Usadel equation. In order to solve the Usadel equation it is convenient to express quasiclassical Green's function \check{g} in terms of Riccati coherence functions $\hat{\gamma}^{R,A}$ and $\hat{\gamma}^{R,A}$ and distribution functions \hat{x}^K and $\hat{\hat{x}}^K$. All these functions are 2×2 matrices in spin space and depend on (x, ε, t) . The corresponding expression for \check{g} can be found in Ref.23 and therefore is not explicitly written here. Riccati coherence and distribution functions obey Riccati-type transport equations²⁴, where the appropriate self energy takes the

form $\check{\Sigma}(x, \varepsilon, t) = h\hat{\sigma}_3 + (1/2\pi\tau_s)\hat{\sigma}_3\check{g}\hat{\sigma}_3$. Here τ_s^{-1} is an inverse magnetic scattering time. As the F layer is supposed to be an alloy, a role of magnetic scattering may be quite important^{20,21}. We assume a presence of the relatively strong uniaxial magnetic anisotropy which prevents mixing of spin-up and spin-down Green's functions, so the magnetic scattering term is a diagonal matrix in spin space²².

The Riccati-type transport equations should be solved together with the boundary conditions at SF interfaces. As it was mentioned above we consider the case when the dimensionless conductance of the boundary $G \equiv R_F/R_g \lesssim 1$, so the interface transparency $T \sim G(l/d) \ll 1$ (l is the mean free path). Due to the smallness of the interface transparency T we can use Kupriyanov-Lukichev boundary conditions at SF boundaries²⁵. In terms of Riccati coherence and distribution functions they take the form

$$2i\pi d \partial_x \hat{\gamma}_{l,r}^R = \pm G \left[\hat{f}_{S;l,r}^R + \hat{\gamma}_{l,r}^R \otimes \hat{g}_{S;l,r}^R - (\hat{g}_{S;l,r}^R + \hat{\gamma}_{l,r}^R \otimes \hat{f}_{S;l,r}^R) \otimes \hat{\gamma}_{l,r}^R \right], \quad (2)$$

$$2i\pi d \partial_x \hat{x}_{l,r}^K = \pm G \left[(1/2) \left(\hat{g}_{S;l,r}^K + \hat{\gamma}_{l,r}^R \otimes \hat{g}_{S;l,r}^K \otimes \hat{\gamma}_{l,r}^A \right) - \hat{\gamma}_{l,r}^R \otimes \hat{f}_{S;l,r}^K - \left(\hat{g}_{S;l,r}^R + \hat{\gamma}_{l,r}^R \otimes \hat{f}_{S;l,r}^R \right) \otimes \hat{x}_{l,r}^K - h.c. \right]. \quad (3)$$

Here Riccati coherence and distribution functions denoted by the lower case symbols l, r are taken at the left and right ends of the ferromagnet. The quantities denoted by the lower case symbols $(S; l, r)$ are corresponding Green's functions at the superconducting side of the left and right SF interfaces. We assume the parameter $(R_F/R_g)(\sigma_F/\sigma_s)$, where σ_F and σ_s stand for conductivities

of ferromagnetic and superconducting materials respectively, to be also small, what allows us to neglect the suppression of the superconducting order parameter in the S leads near the interface and take the Green's functions at the superconducting side of the boundaries to be equal to their bulk values with the appropriate shift of the quasiparticle energy due to the applied voltage

$$V = V_r - V_l.$$

Let us now turn to the analysis of the I-V characteristics.

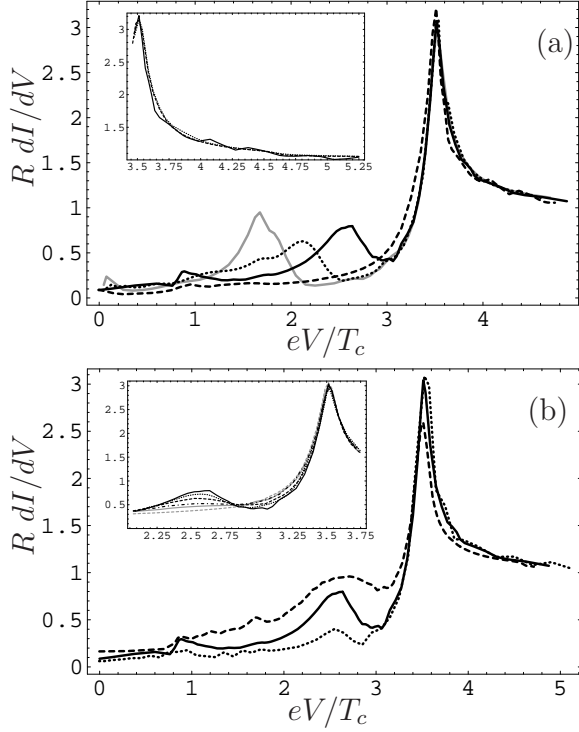


FIG. 1: The zero temperature differential conductance dI/dV , normalized to its value for the normal state of the leads, as a function of eV/T_c , taken for: (a) different exchange fields: $h = 0$ (gray solid); $h = 0.45T_c$ (dotted); $h = 0.9T_c$ (black solid) and $h = 2.6T_c$ (dashed); The inset to (a) shows the RdI/dV as a function of eV/T_c for $h > \Delta$: $h = 2.6T_c$ (solid); $h = 3T_c$ (dashed) and $h = 3.5T_c$ (dotted) are practically undistinguishable; (b) different values of the Thouless energy: $\varepsilon_{Th} = 5T_c$ (dashed); $\varepsilon_{Th} = 2T_c$ (black solid) and $\varepsilon_{Th} = 0.5T_c$ (dotted). T_c is the superconducting critical temperature. $G = 0.1$ and $1/\tau_s = 0$. The inset to (b) demonstrates the influence of the magnetic scattering on the conductance: $1/\tau_s = 0$ (solid); $1/\tau_s = 0.05T_c$ (dotted); $1/\tau_s = 0.15T_c$ (dashed); $1/\tau_s = 0.3T_c$ (dashed-dotted); $1/\tau_s = 0.45T_c$ (gray solid); $1/\tau_s = 0.9T_c$ (gray dashed). $h = 0.9T_c$.

Figure 1(a) shows the dependence of the zero temperature differential conductance dI/dV on voltage for different values of the exchange field in the ferromagnet. The following main features can be observed:

(i) there is a series of peaks at $eV_n = 2\Delta/n$. In fact, only the peaks corresponding to $n = 1, 2$ are seen in the figure. The other harmonics are smeared out due to the small interface transparency and large enough intrinsic broadening of the quasiparticle energy (modelling the inelastic scattering rate) $\gamma = 0.03T_c$, which we take in the numerical calculations. This value of intrinsic broadening is large, but consistent with an estimate of inelastic scattering rate due to electron-phonon processes $\gamma \sim \varepsilon^3/\omega_D^2$ at high enough energies $\varepsilon \sim \Delta^{26}$.

(ii) for $h \lesssim \Delta$ the large additional maximum appears at roughly $eV = \Delta + h$, while the curves corresponding to $h > \Delta$ do not exhibit any additional pronounced characteristic features, in particular at $eV = \Delta + h$ (See Insert to Fig.1(a)). The exchange fields of order of several Δ only result in the suppression of the peak at $eV = \Delta$. In fact, the larger the exchange field the less different from each other the appropriate conductance curves. Of course, this statement is related to the region of weak exchange fields we study.

Analyzing the dependence of the I-V characteristics on the Thouless energy $\varepsilon_{Th} = D/d^2$, which is represented in Figure 1(b), we can conclude, that the most pronounced maximum at $eV \sim \Delta + h$ exists at the region $\varepsilon_{Th} \sim \Delta$. If the Thouless energy increases the peak washes out and finally vanishes. At the limit of very short junction $\varepsilon_{Th} \gg \Delta$ the only structure $eV = 2\Delta/n$ survives. On the other hand, with decreasing the Thouless energy the amplitude of maximum at $eV \sim \Delta + h$ reduces to the zero value at the limit of very small Thouless energies and again the only structure at $eV = 2\Delta/n$ can be observed. With the increasing of transparency of the interfaces the maximum smears out and is masked by the growing peak at $eV = \Delta$.

The inset to Figure 1(b) demonstrates the influence of the magnetic scattering on the maxima discussed above. It can be seen that the magnetic scattering does not influence the peak at $eV = 2\Delta$, while the maximum at $eV \sim \Delta + h$ is broadened, but not dramatically for small compared with T_c values of magnetic scattering rate. Of course, large enough values of $1/\tau_s \sim h, T_c$ destroy the peak and we found the characteristic value of $1/\tau_s$, under which the peak completely washes out, to be approximately equal to $0.45T_c$. The magnetic scattering is typically arises due to the magnetic inhomogeneity, related above all to *Ni*-rich clusters, and can be of order of the average exchange field in the ferromagnetic alloys like $Cu_{1-x}Ni_x$ (see 22 and references therein). However, one can believe that the magnetic inhomogeneity could be weaker in the more diluted alloys with very low exchange fields of order of Δ resulting in small values of magnetic scattering parameter $1/\tau_s$, even compared with T_c .

The appearance of this additional maximum in the intermediate regime $\varepsilon_{Th} \sim \Delta$ is caused by the proximity effect in the ferromagnetic region and can be qualitatively understood as follows. It is well known that for a diffusive SNS junction the zero-bias density of states (DOS) has a minigap in the normal region. For low-transparency junctions it is $\Delta_g \propto G\varepsilon_{Th}$. If the normal metal is replaced by a ferromagnet, the exchange field h shifts the densities of states for the two spin subbands in the opposite directions, therefore the minigap in the spectrum closes at $h \sim \Delta_g^5$, but the sharp onsets in the DOS for the both subbands survive until they merge the edge of the continuous spectrum. So for small enough values of $\Delta_g < h$ and $eV \sim \Delta + h \pm \Delta_g$ an electron belonging to the one spin subband travels through the interlayer from one sharp onset of the DOS at $-\Delta$ to another one

at $h \pm \Delta_g$, while an electron from the other spin sub-band can move from $-h \pm \Delta_g$ to the edge of continuous spectrum at $+\Delta$. According to this qualitative consideration the maximum should be split and the splitting is roughly proportional to the value of the equilibrium minigap $\Delta_g \sim G\varepsilon_{Th}$. We do not observe such splitting at our curves. In addition, due to the multiple Andreev reflection processes there could arise the subsequent harmonics at $eV \sim (\Delta + h \pm \Delta_g)/n$. Of course, the proposed qualitative explanation is very crude because it deals with the equilibrium minigap instead of real position-dependent pseudogap at finite bias and does not take into account the behavior of the distribution function in the interlayer, which is highly nonequilibrium and obviously influences the I-V characteristics.

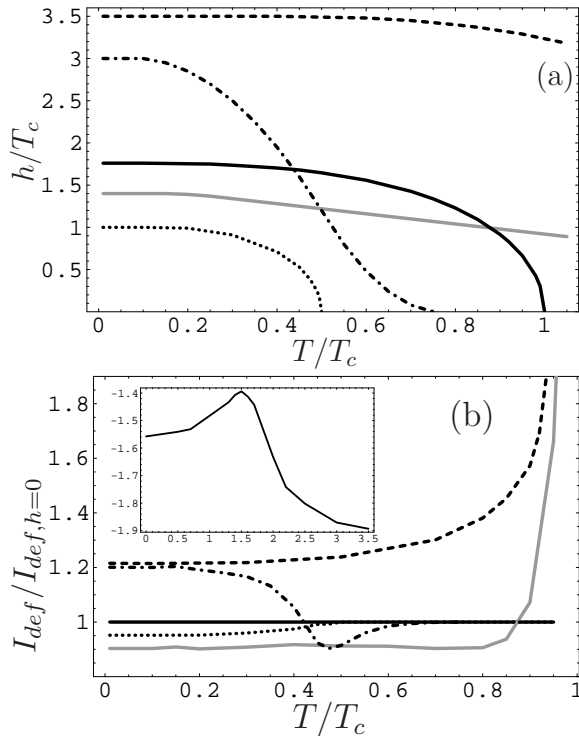


FIG. 2: (a) Possible dependencies of the weak exchange field on temperature. The black solid line represents the BCS-type behavior of $\Delta(T)/T_c$. (b) The appropriate temperature dependencies of the deficit current, normalized to its value at $h = 0$. The inset shows the deficit current eIR/T_c as a function of the exchange field at $T = 0$, $G = 0.1$, $\varepsilon_{Th} = 2T_c$.

Let us now discuss the behavior of the high voltage $eV \gg \Delta$ deficit current $I_{def} = I - V/R < 0$, where $R = R_F + 2R_g$ is the full resistance of the junction. The inset in Figure 2 represents the typical dependence of the deficit current on the exchange field. The deficit current

is a non-monotonous function of the exchange field and reaches a maximum at $h \sim \Delta$. The non-monotonous behavior of the deficit current leads to very peculiar dependencies of this current on temperature. The corresponding curves have the characteristic features determined by the temperature dependence of the exchange field. Figure 2(a) shows several examples of possible behavior of exchange field on temperature in comparison with the temperature dependence of $\Delta(T)$. Figure 2(b) represents the corresponding dependencies of the deficit current on temperature. They are normalized to the value of the deficit current at zero exchange field. It is seen that (i) if $h(T) < \Delta(T)$ in the whole temperature region $0 < T < T_c$, the curve $\tilde{I}_{def}(T) = I_{def}(T)/I_{def,h=0}(T)$ resembles the appropriate dependence $h(T)$ up to the Curie temperature of the ferromagnet T_{Cu} and then follows the curve for $h = 0$ (dotted curve), (ii) in the opposite case of $h(T) > \Delta(T)$ for $0 < T < T_c$ $\tilde{I}_{def}(T)$ monotonously increases up to $T = T_c$ (dashed curve), (iii) if $h(0) > \Delta(0)$ and $T_{Cu} < T_c$, then $\tilde{I}_{def}(T)$ has a minimum approximately at the intersection point of the curves $h(T)$ and $\Delta(T)$. For the temperatures higher than T_{Cu} it follows the curve for $h = 0$ (dashed-dotted curve) and (iv) if $h(0) < \Delta(0)$ and $T_{Cu} > T_c$, then $\tilde{I}_{def}(T)$ grows starting from the values less than that one for $h = 0$, intersects this line and rises very sharply at $T \rightarrow T_c$ (gray solid curve).

In summary, we have developed the theory of the I-V characteristics of diffusive SFS junctions with highly enough resistive SF interfaces. It is found that weak exchange field of the ferromagnet manifests itself only in the coherent regime $\varepsilon_{Th} \sim \Delta$. For $h < \Delta$ it results in the appearance of the additional well-pronounced maximum in the differential conductance at $eV \sim (\Delta + h)$ if the magnetic scattering rate in the ferromagnetic region is small compared to T_c . We have also studied the deficit current at high voltages and found that it behaves non-monotonously as a function of the exchange field exhibiting a maximum at $h \sim \Delta$. This gives rise to the characteristic features in the temperature behavior of the deficit current, determined by the temperature dependence of the exchange field. We believe, that all the discussed features can be measured in the diffusive SFS junctions, realized on the basis of weak ferromagnetic alloys.

We thank V.V. Ryazanov and A. Yu. Rusanov for discussions. The support by RFBR Grants 05-02-17175 (I.V.B. and A.M.B.), 05-02-17731 (A.M.B.) and the programs of Physical Science Division of RAS is acknowledged. I.V.B. was also supported by the Russian Science Support Foundation.

¹ M. Eschrig, J. Kopu, J.C. Cuevas, and G. Schön, Phys.Rev.Lett. **90**, 137003 (2003).

² R.S. Keizer, S.T.B. Goennenwein, T.M. Klapwijk, G. Miao, G. Xiao, and A. Gupta, Nature **439**, 825 (2006).

- ³ A.I. Buzdin, Rev.Mod.Phys. **77**, 935 (2005).
- ⁴ A. Kadigrobov, R.I. Shekhter, M. Jonson, Z.G. Ivanov, Phys.Rev.B **60**, 14593 (1999); A. Kadigrobov, R.I. Shekhter, M. Jonson, cond-mat/0503643.
- ⁵ R. Fazio and C. Lucheroni, Europhys. Lett. **45**, 707 (1999).
- ⁶ A. Martin-Rodero, A. Levy Yeyati, J.C. Cuevas, Physica C, **352**, 117 (2001).
- ⁷ M. Andersson, J.C. Cuevas, M.Fogelström, Physica C, **367**, 117 (2002).
- ⁸ I.V. Bobkova, Phys.Rev.B **73**, 012506 (2006).
- ⁹ Erhai Zhao and J.A. Sauls, cond-mat/0603610.
- ¹⁰ A. Bardas, and D.V. Averin, Phys.Rev. B, **56**, 8518 (1997); A.V. Zaitsev, and D.V. Averin, Phys. Rev. Lett. **80**, 3602 (1998).
- ¹¹ A. Brinkman, A.A. Golubov, H. Rogalla, F.K. Wilhelm, M.Yu. Kupriyanov, Phys. Rev. B **68**, 224513 (2003).
- ¹² A.F. Volkov, A.V. Zaitsev, T.M. Klapwijk, Physica C, **210**, 21 (1993).
- ¹³ T.M. Klapwijk, G.E. Blonder, and M. Tinkham, Physica B+C **109-110**, 1657 (1982).
- ¹⁴ M. Octavio, M. Tinkham, G.E. Blonder, and T.M. Klapwijk, Phys.Rev.B **27**, 6739 (1983); K. Flensberg, J.Bindslev Hansen, and M. Octavio, *ibid.* **38**, 8707 (1988).
- ¹⁵ E.V. Bezuglyi, E.N. Bratus', V.S. Shumeiko, G. Wendin, and H.Takayanagi, Phys. Rev. B, **62**, 14439, (2000); E.V. Bezuglyi, E.N. Bratus', V.S. Shumeiko, G. Wendin, Phys. Rev. B, **63**, 100501, (2001).
- ¹⁶ J.C. Cuevas, J. Hammer, J. Kopu, J.K. Viljas, and M. Eschrig, Phys.Rev.B **73**, 184505 (2006).
- ¹⁷ J. Kutchinsky, R. Taboryski, T. Clausen, C. B. Sorensen, A. Kristensen, P. E. Lindelof, J. Bindslev Hansen, C. Schelde Jacobsen and J. L. Skov, Phys.Rev.Lett. **78**, 931 (1997); J. Kutchinsky, R. Taboryski, O. Kuhn, C. B. Sorensen, P. E. Lindelof, A. Kristensen, J. Bindslev Hansen, C. Schelde Jacobsen and J. L. Skov, Phys.Rev.B **56**, R2932 (1997).
- ¹⁸ T. Hoss, C. Strunk, T. Nussbaumer, R. Huber, U. Staufer and C. Schonenberger, Phys.Rev.B **62**, 4079 (2000).
- ¹⁹ K.D. Usadel, Phys.Rev.Lett. **25**, 507 (1970).
- ²⁰ H. Sellier, C. Baraduc, F. Lefloch, and R. Calemczuk, Phys.Rev. B **68**, 054531 (2003).
- ²¹ V.V. Ryazanov, V.A. Oboznov, A.S. Prokofiev, V.V. Bol'ginov, A.K. Feofanov, Journ. Low Temp. Phys. **136**, 385 (2004).
- ²² V.A. Oboznov, V.V. Bol'ginov, A.K. Feofanov, V.V. Ryazanov, and A.I. Buzdin, Phys.Rev.Lett. **96**, 197003 (2006).
- ²³ M. Eschrig, Phys. Rev. B **61**, 9061 (2000).
- ²⁴ M. Eschrig, J. Kopu, A. Konstandin, J.C. Cuevas, M. Fogelström, and Gerd Schön, Advances in Solid State Physics, **44**, 533 (2004).
- ²⁵ M.Yu. Kupriyanov and V.F. Lukichev, Sov. Phys. JETP **67**, 1163 (1988).
- ²⁶ V.F. Gantmakher, Y.B. Levinson, *Carrier Scattering in Metals and Semiconductors*, Elsevier Science Ltd., 1987.